Self-heating and memory effects in RF power amplifiers explained through electro-thermal

Wei, Wei; Jensen, Ole Kiel; Mikkelsen, Jan H.

Published in:
IEEE Press

DOI (link to publication from Publisher):
10.1109/NORCHIP.2013.6702015

Publication date:
2013

Document Version
Early version, also known as pre-print

Self-heating and Memory Effects in RF Power Amplifiers Explained Through Electro-Thermal Modeling

Wei Wei, Ole Kiel Jensen, Jan H. Mikkelsen

***Abstract*—Self-heating has already been proven to be one of the key sources to memory effects in RF power amplifiers (PAs). However, mechanisms behind the generation of memory effects, as caused by self-heating have not been well documented. On basis of transistor physical properties this paper proposes a simple electro-thermal model and shows how self-heating can generate different types of memory effects, such as bandwidth dependent intermodulation components and hysteresis loops. In addition, it is shown that self-heating can result in generation of new spectral components even in an otherwise linear PA. A time domain modeling framework is implemented to investigate memory effects generated by self-heating and simulation results are shown to agree with theoretical analysis.**

***Index Terms*—Memory effect, self-heating, power amplifier, intermodulation, hysteresis,**

I. INTRODUCTION

Memory effects observed in typical RF PAs normally originate from 3 sources: self-heating [1], electron trapping [2] and baseband effects [1], [3]. Usually, these sources affect the performance of PAs simultaneously, which makes an understanding of the impact of each source difficult. Consequently, PAs with memory effects are normally analyzed and modeled behaviorally on the basis of measured data. For instance, Volterra series [4] represents a typical behavioral modeling approach. However, a behavioral modeling approach does not offer any physical explanation and understanding of the mechanism behind the memory effects.

As a memory source self-heating has been observed to affect intermodulation distortion [1], [5]. In a system with memory, the intermodulation depends not only on signal magnitudes but also on signal bandwidth [6]. This paper shows that bandwidth-dependent intermodulation can be caused by self-heating and clearly explains the physical mechanism behind. The occurrence of AM/AM hysteresis loops is another typical result of memory effects [7]. So far no link between self-heating and AM/AM hysteresis loops has been established in the literature. By adding a simple electro-thermal model this paper forms the link and shows how self-heating can result in AM/AM hysteresis.

Thorough understanding of the generation of memory effects can improve characterization and modeling of PAs. To achieve this, physical properties of transistors need to be investigated. On the basis of these physical properties, this paper explains the mechanism by which self-heating generates bandwidth-dependent output spectral components, AM/AM hysteresis loop opening and dynamic AM/AM and AM/PM behavior. Especially, for the first time, it is detailed how self-heating can be a source to generate AM/AM hysteresis loops and why the loop opening is bandwidth-dependent. The underlying physical reason for these memory effects is the interaction between RF signals and slow thermal responses.

This paper is organized as follows. The electro-thermal response of a class-A PA is discussed in section II, and how an electro-thermal response can generate memory effects is discussed in section III. Conclusions are finally given in section VI.

Wei Wei, Ole Kiel Jensen and Jan H. Mikkelsen are with the Department of Electronic Systems, Aalborg University, Denmark.
Manuscript submitted August 23, 2013

II. ELECTRO-THERMAL RESPONSE IN PAS

The electro-thermal response observed in PAs can be described by means of a feedback loop [8], as illustrated in Fig. 1 where the transistor is simply modelled as a linear but temperature dependent transconductance..

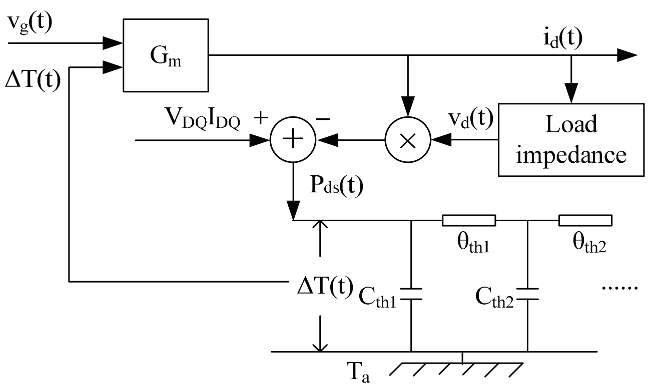

Fig. 1. Interaction between RF signals and thermal response in a FET based PA. $v_g(t)$ denotes the gate voltage, G_m the transconductance, i_d and v_d denote the RF components of the drain current and voltage, I_{DQ} and V_{DQ} represent the drain bias current and voltage, C_{th} and θ_{th} terms denote thermal capacitance and resistance. T_a , P_{ds} and ΔT denotes the ambient temperature, power dissipation and the temperature change respectively.

During operation, both bias and RF signals result in thermal power dissipation. As a consequence, both bias and RF signals affect the FET temperature (T_{FET}). A changing T_{FET} affects G_m, that is, higher T_{FET} normally results in lower G_m following a roughly linear relation between G_m and T_{FET} [9]. By affecting G_m, T_{FET} indirectly interacts with RF signals, which gives rise to the electro-thermal response in a PA. In the following discussion, a simplified linear relation between G_m and T_{FET} is assumed: $G_m = G_{ma} - \gamma\Delta T$, where G_{ma} is the gate transconductance at the ambient temperature and γ is a positive coefficient.

Since P_{ds} is time-varying, the same will be the case for T_{FET}. If a PA is excited by an RF signal with a periodic envelope, T_{FET} can be expressed as

$$T_{FET}(t) = T_a + T_0 + \sum_{n=1}^{N} T_n \cos(n\omega_{th}t + \phi_n), \qquad (1)$$

where T_0 is the DC component of $\Delta T(t)$, $\omega_{th} = \frac{2\pi}{T_e}$ and T_e is the period of the signal envelope. The thermal time constant is normally in the range of μs. Therefore the temperature change within an RF-period is negligible.

Under two-tone excitation, the drain current can thus be expressed as

$$i_d = \{G_{ma} - \gamma[T_0 + \sum_{n=1}^{N} T_n \cos(n(\omega_{th})t + \phi_n)]\} \qquad (2)$$
$$\cdot V_g(\cos\omega_1 t + \cos\omega_2 t),$$

where V_g is the input amplitude of each tone. The power dissipation has spectral components from DC to RF frequencies. Due to the low-pass property of thermal circuits, only DC and baseband components can contribute to T_{FET} variations. Therefore, under two-tone excitation $\omega_{th} = \omega_2 - \omega_1$. In the simplified case of N=1, based on Eq. (2) the drain current is found to be

$$\begin{aligned} i_d &= (G_{ma} - \gamma T_0)V_g \cos\omega_1 t - \frac{1}{2}\gamma T_1 V_g \cos(\omega_1 - \phi_1) \\ &(G_{ma} - \gamma T_0)V_g \cos\omega_2 t - \frac{1}{2}\gamma T_1 V_g \cos(\omega_2 + \phi_1) \\ &- \frac{1}{2}\gamma T_1 V_g \cos(n(2\omega_1 - \omega_2)t - \phi_1) \\ &- \frac{1}{2}\gamma T_1 V_g \cos(n(2\omega_2 - \omega_1)t + \phi_1). \end{aligned} \qquad (3)$$

From Eq. (3) it is shown that the mixing of the two tones and the thermal response causes amplitude and phase distortion of the two tones (first two lines) and also generates 3rd order intermodulation products (last two lines). Both magnitudes and phases of the generated intermodulation products are bandwidth dependent since T_n terms are bandwidth dependent. Secondly, Eq. (2) shows the appearance of AM/AM hysteresis loops. For simplicity, if only T_1 is considered and harmonic terms of T_n are neglected, the input envelope and G_m under this simplified condition are shown in Fig. 2. At the rising and falling edges of the input envelope, all G_m curves are symmetrical while $\phi_n = (2n+1)\pi/2$, but asymmetrical while $\phi_n \neq (2n+1)\pi/2$. Obviously, asymmetry of G_m results in asymmetry of output envelopes.

The T_1 term makes G_m change periodically at ω_{th}. Similarly, a T_n term makes G_m change periodically at $n\omega_{th}$ if $n\omega_{th}$ is below the cut-off frequency of the thermal circuit. Variation of G_m causes distortions to signals.

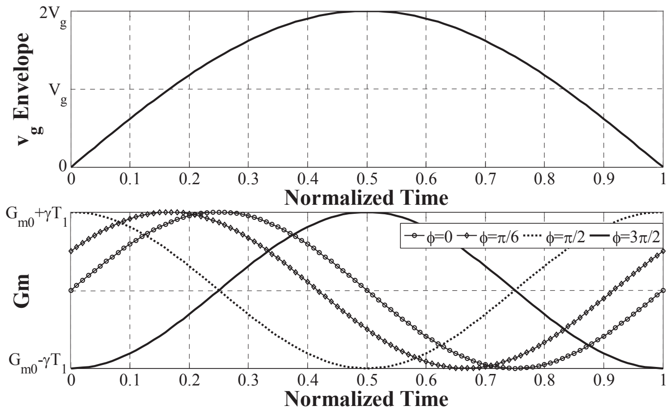

Fig. 2. Claculated input envelope and periodically changing transconductance of a class-A PA under two-tone excitation. The moment at which the envelope is zero is assigned to be zero on the time axis, and the time is normalized to $\frac{2\pi}{\omega_2 - \omega_1}$.

III. Memory Effects Due to Electro-Thermal Response

To investigate memory effects, a class-A PA model is implemented in Matlab Simulink with the modeling framework in Fig. 1. This model is implemented on the basis of a 20-finger FET. The gate width of each finger is $50\mu\mathrm{m}$ and the parameters of each finger are described by [9]. For this FET, the parameters at $T_a = 325$ K and $V_{GQ} = -4.5$ V are $G_{ma} \approx 0.12$ S and $\gamma \approx 0.0002$ S/K. With this FET the simulation is based on the following parameters: $G_{ma} = 0.12\,\mathrm{S}$, $\gamma = 0.0002\,\mathrm{S/K}$, $V_{DQ}I_{DQ} = 6$ W, load impedance = 50 Ω, $\theta_{th} = 40$ K/W, $C_{th} = 1.25 \times 10^{-6}$ J/K.

Two-tone signals and stepped signals are introduced to excite the PA. The centre frequency of the RF signal during the simulation is 1 GHz.

A. T_{FET} *under Two Tone Excitation*

Fig. 3 shows that under two tone excitation, ΔT changes periodically at the period of $2\pi/(\omega_2 - \omega_1)$, and T_n harmonics appear. However, under single tone excitation, ΔT is a constant value.

It is interesting to see that both the magnitude and phase of ΔT depend on the difference frequency, $\omega_2 - \omega_1$. This is due to the low-pass properties of the thermal circuit. Fig. 4 shows the frequency response of the thermal impedance, where $Z_{th} = \theta_{th}/(j\omega_{th}C_{th} + 1)$ denotes the thermal impedance.

B. *Intermodulation Generated by Self-heating*

Intermodulation products under two tone test appear in output signals, which is shown to agree with Eq. (2). Magnitudes of these components depend on the difference frequency of the two tones, as is shown in Fig. 5.

Demonstrated in Fig. 4 and 5, both magnitudes of IMD3 and Z_{th} decrease as the difference frequency increases. The underlying physical reason is that a higher magnitude of Z_{th} cause higher magnitudes of T_n terms, and hence higher magnitudes of intermodulation components, as illustrated by Eq. (2).

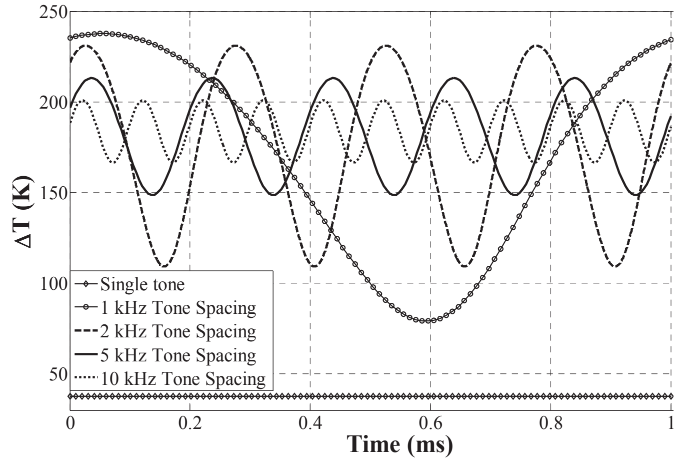

Fig. 3. Simulation results of ΔT due to self-heating in a Class-A PA at $V_g = 2\,\mathrm{V}$.

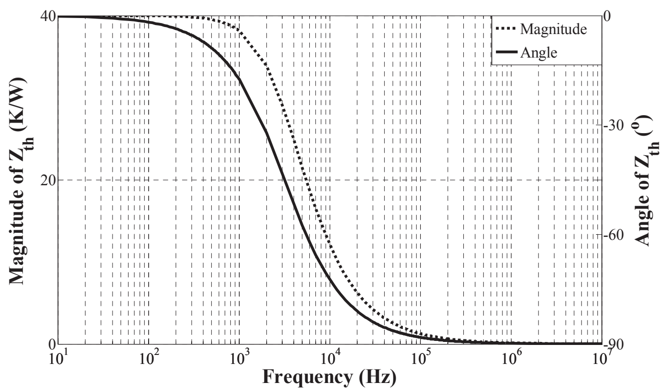

Fig. 4. Calculated thermal impedance of the FET with $\theta_{th} = 40\,\mathrm{K/W}$ and $C_{th} = 1.25 \times 10^{-6}$ J/K.

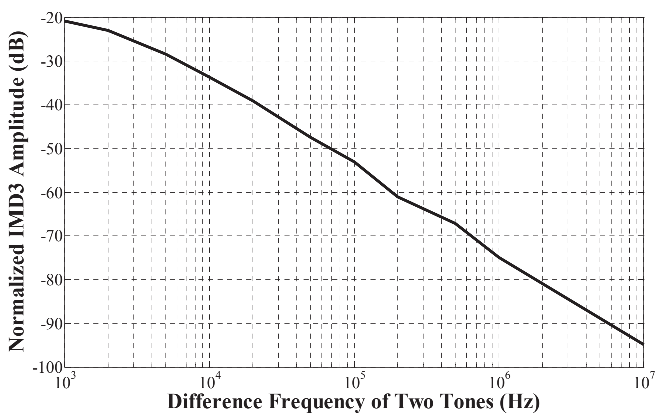

Fig. 5. Simulated IMD3 magnitude vs. difference frequency at $V_g = 2$ V . IMD3 magnitudes are normalized to the magnitude of the fundamental tones.

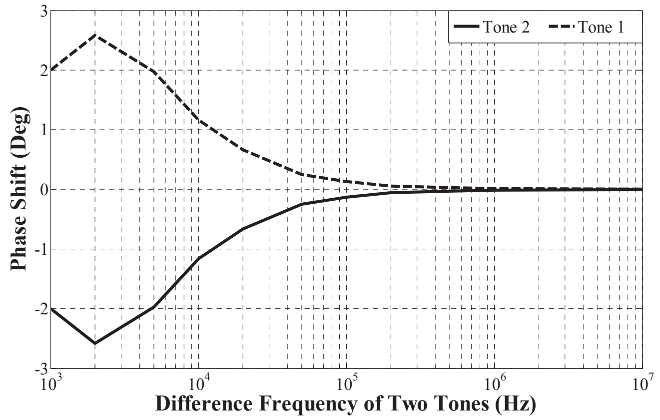

Fig. 6. Simulated phase shift due to self-heating vs. difference frequency of two tones at $V_g = 2\,\mathrm{V}$.

C. Phase Variation

The phase shift of the two output tones is also bandwidth-dependent, as shown in Fig. 6. When the difference frequency is outside the pass band of the thermal circuit, self-heating cannot cause phase variation to the two output tones.

D. AM/AM Characteristic

Fig. 7 shows output envelopes and ΔT. The asymmetry of the output envelopes is due to the asymmetry of T_{FET}. Fig. 8 shows AM/AM hysteresis loops. In these 2 figures, the v_g envelope is normalized to $2V_g$, and i_d envelopes are normalized to their maximum values, that is, 0.41 A, 0.38 A, 0.34 A, 0.33 A. The difference frequencies of the two tones are 1 kHz, 2 kHz, 10 kHz, 50 kHz, respectively.

The size of an AM/AM hysteresis loop depends on both magnitude and angle of Z_{th}, and then the loop-opening is also bandwidth-dependent, as is shown in Fig. 8.

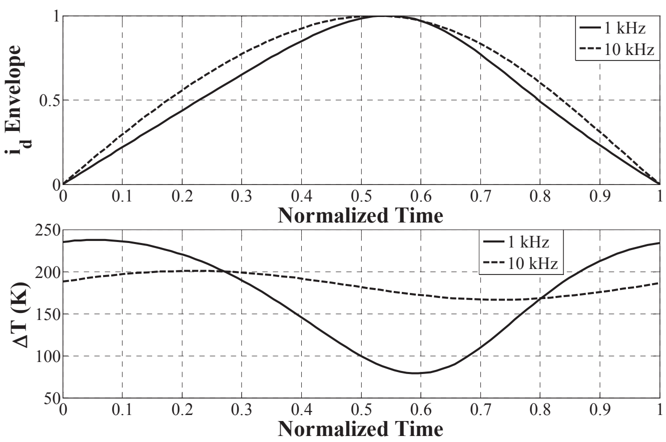

Fig. 7. Simulation results of output envelopes and ΔT in a half of the envelope period at $V_g = 2$ V. For each tone spacing, time starts at a zero point of the envelope and normalized to $\frac{2\pi}{\omega_2 - \omega_1}$.

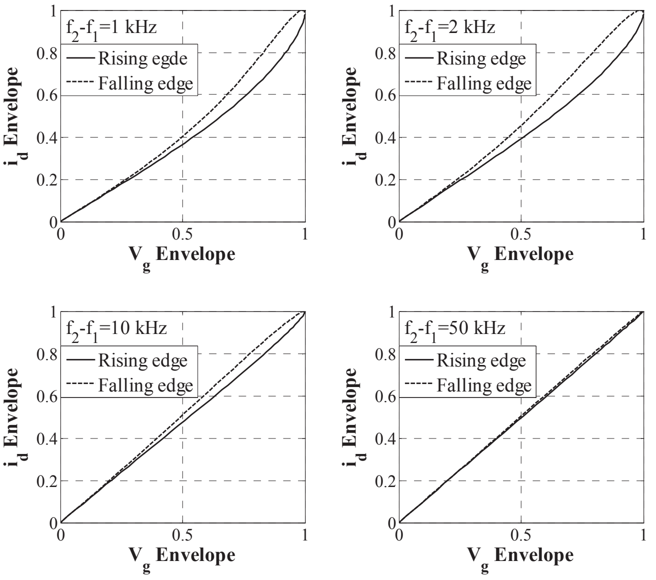

Fig. 8. Simulation results of AM/AM hysteresis loop opening caused by self-heating at $V_g = 2\,\mathrm{V}$. Input and output envelopes are normalized to their maximum values respectively.

E. Response to Stepped RF signal

Fig. 9 shows that under step single-tone excitation, at the rising edges of the input envelope, the output envelope rises exponentially while T_{FET} drops exponentially. In addition, at the falling edges of the input envelope, the output envelope drops exponentially while T_{FET} rises exponentially.

The step response of the output envelope is due to the thermal response of the FET. Due to this step response, the output signal magnitude depends not only on the present input but also on the previous input.

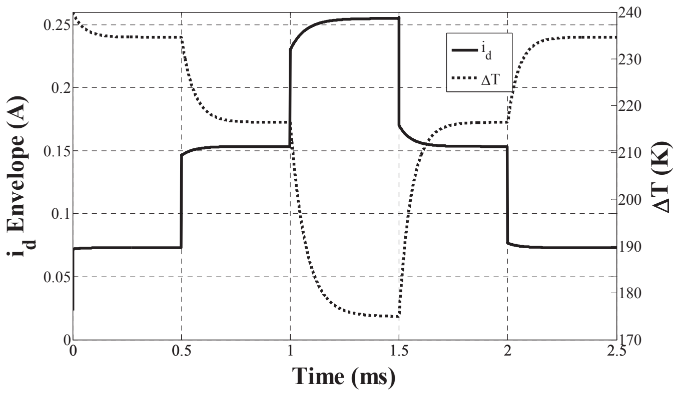

Fig. 9. Simulation results of output envelope and ΔT under step single-tone excitation. V_g starts at 0 V, steps to 1 V at 0 ms, to 2 V at 0.5 ms, to 3 V at 1 ms, to 2 V at 1.5 ms and to 1 V at 2 ms.

IV. Conclusion

On the basis of physical properties of FETs, this paper explains how self-heating can cause memory effects in an RF PA. Thermal properties of FETs have low pass characteristics. Under two-tone excitation, while the difference frequency is lower than the cut-off frequency of the low-pass thermal circuit, the FET temperature and hence the transconductance changes periodically at the difference frequency. This periodically changing transconductance generates new spectral components, causes AM/AM hysteresis loop opening, and introduces magnitude and phase variation to output signals. All these effects are bandwidth dependent and disappear while the difference frequency is outside the pass band of the thermal circuit. Under stepped single-tone excitation, the thermal response causes an exponential increase and decrease of the output envelope.

Simple mathematics is formulated to describe the mechanism by which self-heating generates memory effects. As an outcome of the theoretical analysis, a time domain modeling framework is proposed and implemented. Simulation results are shown to agree with the theoretical analysis.

References

[1] N. Le Gallou, J. Nebus, E. Ngoya, and H. Buret, "Analysis of low frequency memory and influence on solid state HPA intermodulation characteristics," in *Microwave Symposium Digest, 2001 IEEE MTT-S International*, vol. 2, 2001, pp. 979 –982 vol.2.

[2] G. Meneghesso, G. Verzellesi, R. Pierobon, F. Rampazzo, A. Chini, U. Mishra, C. Canali, and E. Zanoni, "Surface-related drain current dispersion effects in AlGaN-GaN HEMTs," *Electron Devices, IEEE Transactions on*, vol. 51, no. 10, pp. 1554 – 1561, oct. 2004.

[3] N. Borges de Carvalho and J. Pedro, "A comprehensive explanation of distortion sideband asymmetries," *Microwave Theory and Techniques, IEEE Transactions on*, vol. 50, no. 9, pp. 2090 – 2101, sep 2002.

[4] A. Zhu and T. Brazil, "Behavioral modeling of RF power amplifiers based on pruned volterra series," *Microwave and Wireless Components Letters, IEEE*, vol. 14, no. 12, pp. 563 – 565, dec. 2004.

[5] J. Vuolevi and T. Rahkonen, "Analysis of third-order intermodulation distortion in common-emitter BJT and HBT amplifiers," *Circuits and Systems II: Analog and Digital Signal Processing, IEEE Transactions on*, vol. 50, no. 12, pp. 994 – 1001, dec. 2003.

[6] J. Vuolevi, T. Rahkonen, and J. Manninen, "Measurement technique for characterizing memory effects in RF power amplifiers," *Microwave Theory and Techniques, IEEE Transactions on*, vol. 49, no. 8, pp. 1383 –1389, aug 2001.

[7] N. Wolf, J.-E. Mueller, and H. Klar, "Identification of frequency dependent memory effects and the linearization of a cmos pa for multiple standards," in *Radio and Wireless Symposium, 2009. RWS '09. IEEE*, jan. 2009, pp. 598 –601.

[8] A. Parker and J. Rathmell, "Broad-band characterization of FET self-heating," *Microwave Theory and Techniques, IEEE Transactions on*, vol. 53, no. 7, pp. 2424 – 2429, july 2005.

[9] R. Gaska, Q. Chen, J. Yang, A. Osinsky, M. Asif Khan, and M. Shur, "High-temperature performance of AlGaN/GaN HFETs on SiC substrates," *Electron Device Letters, IEEE*, vol. 18, no. 10, pp. 492 –494, oct 1997.